



ELSEVIER

Journal of Power Sources 97–98 (2001) 415–419

JOURNAL OF
POWER
SOURCES

www.elsevier.com/locate/jpowersour

Preparation of lithium manganese oxides containing iron

Mitsuharu Tabuchi^{a,*}, Hikari Shigemura^a, Kazuaki Ado^a, Hironori Kobayashi^a,
Hikari Sakaebe^a, Hiroyuki Kageyama^a, Ryoji Kanno^b

^aOsaka National Research Institute, 1-8-31 Midorigaoka Ikeda, Osaka 563-8577, Japan

^bKobe University, 1-1 Rokko-dai, Nada, Kobe, Hyogo 657, Japan

Received 27 June 2000; received in revised form 3 January 2001; accepted 13 January 2001

Abstract

Preparation of $\text{LiFeO}_2\text{--Li}_2\text{MnO}_3$ solid solution has been attempted using hydrothermal and solid state reactions. Three 10% Fe-doped Li_2MnO_3 samples ($\text{Fe}/(\text{Fe} + \text{Mn}) = 0.1$) with different average particle sizes could be obtained by both methods. The initial charge capacities for these cathodes were sensitive to the preparation method; the capacity up to 4.3 V is 45 mAh/g for the hydrothermally-obtained sample, 24 mAh/g for the post-annealed sample after hydrothermal-treatment at 673 K, and 6 mAh/g for the sample obtained by solid state reaction at 1173 K. ^{57}Fe Mössbauer spectra detect the oxidation of Fe^{3+} to Fe^{4+} /reduction of Fe^{4+} to Fe^{3+} after initial charging/discharging for the hydrothermally obtained sample. The observed $\text{Fe}^{3+/4+}$ redox voltage is between 4.0 and 4.5 V which is lower than that predicted (5 V) for Fe-doped LiMn_2O_4 . This suggests that hydrothermally synthesized Fe-doped Li_2MnO_3 is an environmentally-friendly candidate as cathode material, involving a $\text{Fe}^{3+/4+}$ redox reaction for rechargeable lithium batteries. © 2001 Elsevier Science B.V. All rights reserved.

Keywords: Lithium batteries; $\text{LiFeO}_2\text{--Li}_2\text{MnO}_3$; Hydrothermal reaction

1. Introduction

Lithium iron oxides, LiFeO_2 including metastable polymorphs, are amongst the most attractive cathode materials for large-scale lithium-ion batteries due to the natural abundance of iron. Kanno et al. [1] and Sakurai et al. [2] have succeeded in preparing electrochemically-active LiFeO_2 with corrugated-layered and Goethite-type structures by “soft chemistry” methods (ion-exchange reaction); Guenne et al. [3] have reported the formation of Fe^{4+} ions by electrochemical oxidation. The $\text{Fe}^{3+}/\text{Fe}^{4+}$ redox couple was observed in cathodes of Fe-doped LiNiO_2 [4] and LiCoO_2 [5], while LiFeO_2 with $\alpha\text{-NaFeO}_2$ type structure is almost electrochemically inactive [6]. These reports raise the question as to whether or not Fe^{3+} can be oxidized independently without the oxidation of other cations. We thus, try here to prepare Fe-doped Li_2MnO_3 to observe the $\text{Fe}^{3+}/\text{Fe}^{4+}$ redox behavior in the electrochemically inactive Li_2MnO_3 phase, which has a layered rock-salt structure similar to LiCoO_2 .

2. Experimental

The Fe-doped Li_2MnO_3 samples were obtained by hydrothermal reaction of Fe–Mn coprecipitate (2.7 g, $\text{Fe}/(\text{Fe} + \text{Mn}) = 0.1$ and 0.2) with $\text{LiOH}\cdot\text{H}_2\text{O}$ (10 g, Wako Pure Chem.) and oxidant, KClO_3 (10 g, Wako Pure Chem.) at 493–513 K for 10–240 h using an autoclave (150 cm^3 inner volume) including 50 ml of distilled water. The Fe–Mn coprecipitate was obtained by bubbling air through the precipitate (3–7 days), which was made by adding dropwise NaOH solution to mixed $\text{Fe}(\text{NO}_3)_3\text{--Mn}(\text{NO}_3)_2$ ($\text{Fe}/(\text{Fe} + \text{Mn}) = 0.1$ and 0.2) one.

Undoped Li_2MnO_3 could be obtained by hydrothermal reaction from a mixture of $\text{MnCl}_2\cdot 4\text{H}_2\text{O}$ (4.95 g, Kishida Chem.), $\text{LiOH}\cdot\text{H}_2\text{O}$ (50 g), KOH (120 g, Wako Pure Chem.), and KClO_3 (50 g) at 493 K for 48 h. $\text{Li}_{2-x}\text{MnO}_{3-x/2}$ (non-stoichiometric Li_2MnO_3 prepared below 773 K [7]) were obtained by hydrothermal reaction from a mixture of EMD- MnO_2 (1 g Tosoh Corp.) and $\text{LiOH}\cdot\text{H}_2\text{O}$ (50 g) with 200 ml of distilled water at 493 K for 5 h. These samples were used as undoped materials.

The hydrothermally synthesized samples were washed repeatedly with distilled water and filtered to eliminate the residual salt from the products, and then dried at 373 K. Post-annealing was performed for two kinds of hydrother-

* Corresponding author. Tel.: +81-727-51-9618; fax: +81-727-51-9714.
E-mail address: tabuchi@onri.go.jp (M. Tabuchi).

mally-synthesized samples (673 K for Fe-doped Li_2MnO_3 , and 773 K for $\text{Li}_{2-x}\text{MnO}_{3-x/2}$).

Solid state reaction was used for the Fe-doped sample preparation. To obtain the starting mixture, an aqueous solution of lithium hydroxide was added dropwise to a mixture of $\text{Fe}(\text{NO}_3)_3$ and $\text{Mn}(\text{NO}_3)_2$ ($\text{Fe}/(\text{Fe} + \text{Mn}) = 0.1$) and then used as lithium source ($\text{Li}/(\text{Fe} + \text{Mn}) = 2.00$). After drying at 373 K, Fe–Mn coprecipitate including Li was fired between 773 and 1273 K in air.

The samples were characterized by X-ray diffractometry (XRD, Rigaku Rotaflex RU-200B/RINT) using monochromatic Cu $K\alpha$ radiation (Both Cu $K\alpha_1$ and Cu $K\alpha_2$ reflections were observed in each XRD pattern.). Si powder was used to calibrate 2θ angles ($>10^\circ$). The XRD data were collected for 2 s at each 0.02° step over a 2θ range from 10 to 120° for Rietveld analysis. Reflection positions and intensities were calculated for both Cu $K\alpha_1$ and Cu $K\alpha_2$ reflections. A pseudo-Voigt profile function was used. Particle sizes and shape were checked by transmission electron microscope (TEM). The Li, Mn, Fe and K contents in the obtained solids were determined by inductively coupled plasma (ICP) emission spectroscopy. Mn K-edge XANES spectra were obtained in the transmission mode with an X-ray spectrometer, EXAC-800 (Technos) at 293 K. The X-ray generator with a Mo rotating anode and a LaB_6 cathode was operated at a voltage of 20 kV and an average current of 70 mA. The incident X-ray beam was monochromatized with a $\text{Ge}(4\ 0\ 0)$ Johansson curved crystal. The intensity of the X-ray beam was measured by a solid state detector for both the incident and the transmitted X-ray. ^{57}Fe Mössbauer spectra were recorded at room temperature (Model 222B, Topologic Systems), and $\alpha\text{-Fe}$ was used for velocity calibration. Observed spectra were fitted to peaks with a Lorentzian line-shape.

Electrochemical lithium deintercalation/intercalation reactions were carried out using lithium coin-type cells. The working electrode consisted of a mixture of 20 mg the sample, 5 mg acetylene black, and 0.5 mg Teflon powders pressed into a tablet of 15 mm diameter under a pressure 0.5 MPa. The electrochemical test cells were constructed in a stainless steel coin-type configuration. The negative electrode was a 15 mm diameter and 0.2 mm thick disk of Li foil. The separator was a microporous polypropylene sheet. Typical electrolyte was 1 M solutions of LiClO_4 in a 50:50 mixture of ethylene carbonate (EC) and 1,2-dimethylcarbonate (DMC) by volume (Tomiya Pure Chemical Industries Ltd., battery grade). The water content of the electrolytes was 20 ppm. Cells were constructed in an argon-filled glove-box, and electrochemical measurements were carried out at room temperature after standing overnight on open circuit. The cell properties were measured galvanostatically using a TOSCAT-3100 (Toyo System). After electrochemical testing, the Fe-doped Li_2MnO_3 electrodes were subjected to X-ray diffraction measurement and Mn K-edge XANES spectroscopy without washing and drying. For the ^{57}Fe Mössbauer spectroscopic measurement,

the lithium cells sealed by Al-polymer laminates were used to avoid any degradation of the electrode by disassembling the cell for each measurement.

3. Results and discussion

Three samples (10% Fe-doped Li_2MnO_3) obtained by the different preparation route from the Fe–Mn coprecipitate ($\text{Fe}/(\text{Fe} + \text{Mn}) = 0.1$) gave similar XRD patterns to those of $\text{Li}_{2-x}\text{MnO}_{3-x/2}$ and Li_2MnO_3 (Fig. 1). No other lithium manganese oxides, lithium iron oxides, manganese oxides and iron oxides were detected in these patterns. Chemical analysis showed that the $\text{Fe}/(\text{Fe} + \text{Mn})$ ratio for all samples was 0.10(1), and $\text{Li}/(\text{Fe} + \text{Mn})$ ratios were 1.69(3) for hydrothermally synthesized (493 K, 192 h), 1.68(2) for post-annealed (673 K, 12 h) and 2.00(1) for solid state reaction synthesized (1173 K, 24 h) samples. This means that the samples belong to the $\text{Li}_2\text{MnO}_3\text{--LiFeO}_2$ solid solution rather than $\text{LiMnO}_2\text{--LiFeO}_2$. The average particle sizes of three 10% Fe-doped Li_2MnO_3 samples increased with increasing preparation temperature; 0.2 μm for hydrothermal synthesis, 0.3 μm for annealed, and 0.5 μm for solid state reaction synthesized sample.

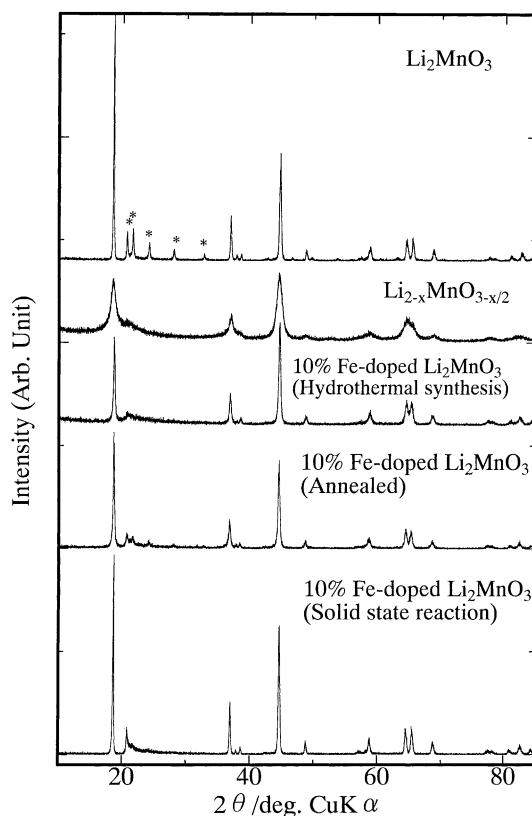


Fig. 1. X-ray diffraction patterns for three Fe-doped Li_2MnO_3 samples with $\text{Fe}/(\text{Fe} + \text{Mn}) = 0.1$ and Li_2MnO_3 and $\text{Li}_{2-x}\text{MnO}_{3-x/2}$. The appearance of five peaks marked by asterisks corresponds to the development of Mn^{4+} hexagonal network for the monoclinic Li_2MnO_3 .

Although both $\text{Li}_{2-x}\text{MnO}_{3-x/2}$ and Li_2MnO_3 have layered rock-salt type structures like LiCoO_2 ($(\text{Li})_{3a}(\text{Mn}, \text{Li})_{3b}\text{O}_2$), the difference is the degree of cation ordering in the Mn–Li mixed cation (Mn_2Li) layer; an Mn^{4+} hexagonal network is observed for Li_2MnO_3 , and is insufficiently developed for $\text{Li}_{2-x}\text{MnO}_{3-x/2}$. Five XRD peaks between 20 and 35° (asterisks on the peaks for Li_2MnO_3) could be developed due to the hexagonal network. An XRD pattern for the hydrothermally and solid state reaction synthesized samples are similar to $\text{Li}_{2-x}\text{MnO}_{3-x/2}$ rather than to monoclinic Li_2MnO_3 . The XRD pattern for the two samples could, thus, be fitted by the unit-cell of $\alpha\text{-NaFeO}_2$ ($R\bar{3}m$, $a = 2.85572(9)$ Å, $c = 14.2187(6)$ Å for hydrothermally synthesized and $a = 2.85026(7)$ Å, $c = 14.2407(4)$ Å for solid state reaction synthesized samples) except for the broad peaks due to the monoclinic distortion at $2\theta = 20$ – 25 , 42 and 58° , indicating that the Fe ions occupy both Li and Mn sites in the Mn_2Li layer. Applying a $(\text{Li}, \text{M})_{3a}(\text{M}, \text{Li})_{3b}\text{O}_2$ model instead of the $(\text{Li})_{3a}(\text{M}, \text{Li})_{3b}\text{O}_2$ model (M: Mn, Fe) gives an improvement agreement (R_{wp} falls from 15.8 to 14.9%) for hydrothermally synthesized sample. The Fe and/or Mn occupation in the lithium layer was estimated to be 3.0(1)%. However, the difference between R_{wp} values for the two models (M: Mn, Fe) is insignificant (19.21 and 19.39%, respectively) for the solid state reaction synthesized sample, indicating the difficulty in detecting transition metals in the Li layer.

The 10% Fe-doped Li_2MnO_3 isostructural with monoclinic Li_2MnO_3 was obtained by post-annealing the hydrothermally synthesized sample at 673 K. The XRD pattern could be fitted to a monoclinic unit cell ($C2/m$,

$a = 4.9264(5)$ Å, $b = 8.5246(6)$ Å, $c = 5.0161(3)$ Å, $\beta = 109.266(7)^\circ$). A change in lattice parameters could be detected compared to undoped Li_2MnO_3 ($a = 4.9307(3)$ Å, $b = 8.5313(4)$ Å, $c = 5.0230(2)$ Å, $\beta = 109.343(4)^\circ$), indicating the formation of the LiFeO_2 – Li_2MnO_3 solid solution. The Fe and/or Mn occupation in the lithium layer was estimated to be 3.2(3)%. XRD pattern fitting of two 20% Fe-doped samples (hydrothermally-synthesized and annealed at 673 K) failed. Only the peak position could be refined to give lattice parameters ($R\bar{3}m$, $a = 2.8648(2)$ Å, $c = 14.2240(18)$ Å) for a hydrothermally synthesized sample. Attempts to obtain more highly crystalline samples by selecting higher annealing temperature were unsuccessful due to the formation of an inverse spinel (LiFe_5O_8) at 723 K. The three 10% Fe-doped samples were used for further characterizations.

The Mn K-edge XANES spectra for hydrothermally synthesized and annealed samples were almost the same for Li_2MnO_3 , indicating that the valence state of Mn was mainly 4+ after Fe doping. Each ^{57}Fe Mössbauer spectrum for the two samples could be fitted by two overlapping doublets with isomer shifts (IS) of +0.30 to 0.35 mm/s at 300 K (Fig. 2), which is typical of high-spin Fe^{3+} compounds such as $\alpha\text{-LiFeO}_2$ (+0.36 mm/s) and $\alpha\text{-NaFeO}_2$ (+0.37 mm/s). The observed spectrum for solid state reaction synthesized sample is an asymmetric doublet with a shoulder around -0.3 mm/s. The two doublets with different IS values (+0.327(3) and $-0.082(14)$ mm/s (93:7 in area ratio)) are needed for the fitting. Although the IS value of the major doublet is close to that of the high-spin Fe^{3+} compounds, the value for the minor doublet is close to the Fe^{4+}

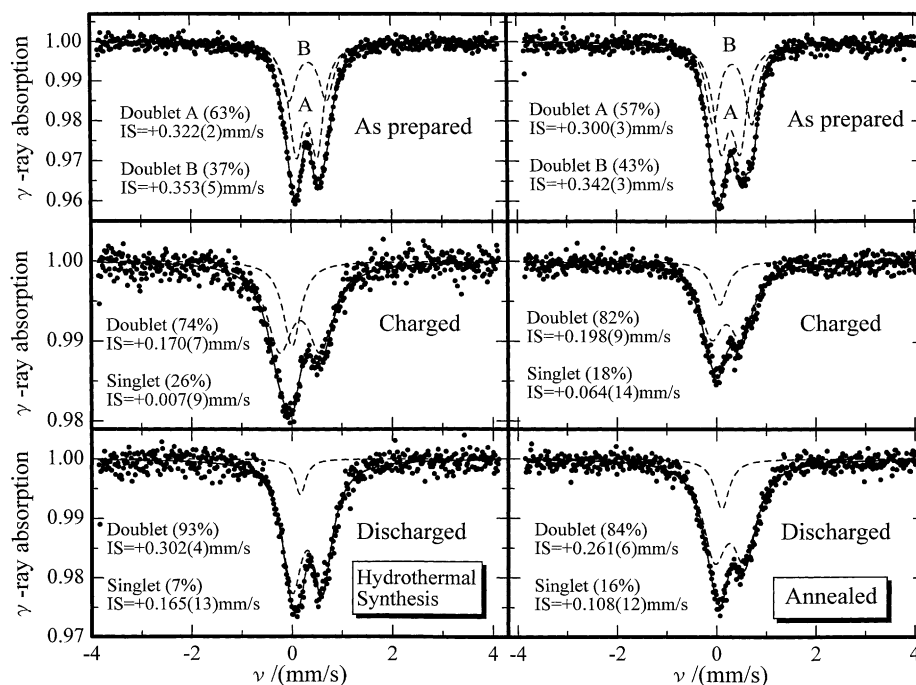


Fig. 2. ^{57}Fe Mössbauer spectra for as-prepared, first-charge, and discharged samples obtained by a hydrothermal reaction and a post-annealing method.

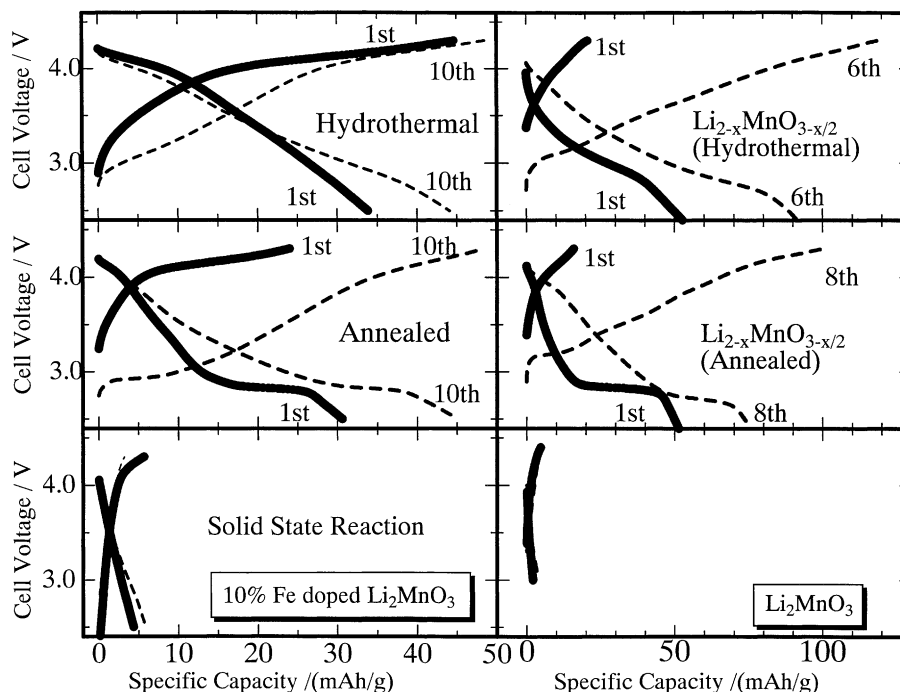


Fig. 3. Charge and discharge profiles of Li/Fe-doped and undoped sample cells. The solid line consists of closed circles and the broken line is the curve for the 1st and 6–10th cycles. The current density is 7.5 mA/g for three Fe-doped samples.

component (-0.1 mm/s) into Fe-doped LiNiO_2 [4]. This suggests the partial oxidation of trivalent iron. These spectroscopy data support that the samples lie on Li_2MnO_3 – LiFeO_2 solid-solution tie line.

Initial and 10th charge and discharge curves for Li/sample cells are shown for the undoped samples in Fig. 3. The Li/solid state reaction synthesized sample cell has negligibly small charge/discharge capacity (<10 mAh/g) at both 1st and 10th cycles, which is similar to the Li/ Li_2MnO_3 cell. The first and 10th discharge and 10th charge profiles of other two samples were similar to the Li/ $\text{Li}_{2-x}\text{MnO}_{3-x/2}$ cells, indicating that partial reduction and re-oxidation of Mn between $4+$ and $3+$ occurred after the first discharge. However, the initial charge capacity for the hydrothermally synthesized sample is difficult to explain only by comparison with the Li/ $\text{Li}_{2-x}\text{MnO}_{3-x/2}$ cells and initial valence state of Mn ($4+$ state). In fact, the Mn K-edge XANES spectrum for the charged sample overlaps with that of the as-prepared sample. The change in valence state for iron after the electrochemical charge/discharge states was observed by ^{57}Fe Mössbauer spectroscopy (Fig. 2). The observed spectra after first-charge are considered to be an asymmetric doublet and could, therefore, be fitted to overlapping a doublet and a singlet. Two possible oxidation states of iron are deduced from the IS values of the doublets; the first is Fe^{3+} tetrahedrally-coordinated by oxide ions like in an inverse spinel structure (LiFe_5O_8 or $\gamma\text{-Fe}_2\text{O}_3$); second possibility is a $3+/4+$ mixed-valence state for Fe on an octahedral site [4]. Although we cannot exclude either possibilities at present, the second is more likely due to the coexistence of the singlet

with IS value (0 mm/s) close to that for an Fe^{4+} ions (singlet: $+0.06$ mm/s of IS value) on an octahedral sites in $\text{SrFeO}_{2.97}$ [8]. The Mössbauer spectra reveal the oxidation of Fe to be from $3+$ to $3 + \delta$ ($0 < \delta < 1$) after charging. The IS values for the doublet and singlet for each sample move to higher values after discharging. The IS values for these doublets are close to those for as-prepared samples and LiFeO_2 . The IS values for the singlet move to the typical value of $\text{Fe}^{3.5+}$ [4] from Fe^{4+} , and the fraction of the singlets decreased compared to that for the charged state. The change in spectra after discharge implies the reduction of some $\text{Fe}^{3+\delta}$ ions to Fe^{3+} . No high-spin Fe^{2+} doublet with relatively large IS value (IS = $+1.07$ mm/s for FeTiO_3 [9]) were observed for both samples, which could be observed by the electrochemical reduction of Fe^{3+} ions in $\text{Li}_x\text{Fe}_2(\text{MoO}_4)_3$ ($0 < x < 2$ at 3.0 V) and $\text{Li}_x\text{Fe}_2(\text{SO}_4)_3$ ($0 < x < 2$ at 3.6 V) [10]. The Mössbauer spectroscopy indicate that no $\text{Fe}^{2+/3+}$ redox couple was involved between 2.5 and 4.3 V and the $\text{Fe}^{3+/4+}$ redox couple was involved in the initial charge and discharge curves for the two samples. The first-charge curve above 4 V is due mainly to the oxidation of Fe^{3+} ion to Fe^{4+} . The reduction voltage from Fe^{4+} to Fe^{3+} is close to 4 V for the hydrothermally synthesized sample, because the change in the fractional area of the singlet and doublet from charged to discharged states is more clearly observed compared to that for the annealed sample, and no 4 V plateau was observed for a Li/hydrothermally synthesized $\text{Li}_{2-x}\text{MnO}_{3-x/2}$ cell. The differences in initial charge and discharge capacities above 4 V for three Fe-doped samples reveal the importance of selecting a low-temperature preparation route; maximum

capacities for initial charge and discharge runs could be obtained for the hydrothermally synthesized sample with the low crystallinity and low average particle sizes.

In conclusion, preparation of a low crystallinity sample using “soft chemistry” methods and partial occupation of iron in the transition metal layer may be a key strategy in the material design of Fe-doped LiMO_2 with $\alpha\text{-NaFeO}_2$ type structure having a $\text{Fe}^{3+/4+}$ redox potential below 5 V. The lowering of redox voltage has been attractive in practical application because the predicted $\text{Fe}^{3+/4+}$ redox potential for Fe-doped LiMn_2O_4 is close to 5 V; such a high voltage leads to decomposition of the organic electrolyte. Further Fe doping into Li_2MnO_3 using hydrothermal reaction is currently in progress.

References

- [1] R. Kanno, T. Shirane, Y. Kawamoto, Y. Takeda, M. Takano, M. Ohashi, Y. Yamaguchi, *J. Electrochem. Soc.* 143 (1996) 2435.
- [2] Y. Sakurai, H. Arai, S. Okada, J. Yamaki, *J. Power Sources* 68 (1997) 711.
- [3] L.B. Guenne, P. Deniard, A. Lecerf, P. Biensan, C. Siret, L. Fournes, R. Brec, *J. Mater. Chem.* 9 (1999) 1127.
- [4] C. Delmas, M. Menetrier, L. Croguennec, I. Saadoune, A. Rougier, C. Pouillier, G. Prado, M. Grune, L. Fournes, *Electrochim. Acta* 45 (1999) 243.
- [5] H. Kobayashi, H. Shigemura, M. Tabuchi, H. Sakaebe, K. Ado, H. Kageyama, A. Hirano, R. Kanno, M. Wakita, S. Morimoto, S. Nasu, *J. Electrochem. Soc.* 147 (3) (2000) 960.
- [6] K. Ado, M. Tabuchi, H. Kobayashi, O. Nakamura, Y. Inaba, R. Kanno, M. Takagi, Y. Takeda, *J. Electrochem. Soc.* 144 (1997) L177.
- [7] M.M. Thackeray, *Prog. Solid State Chem.* 25 (1997) 1.
- [8] Y. Takeda, R. Kanno, T. Takada, O. Yamamoto, M. Takano, N. Nakayama, Y. Bando, *J. Solid State Chem.* 63 (1986) 237.
- [9] E. Murad, J.H. Johnston, Iron oxides and oxyhydroxides, in: G.J. Long (Ed.), *Mössbauer Spectroscopy Applied to Inorganic Chemistry*, Vol. 2, Modern Inorganic Chemistry Series, Plenum Press, New York, 1987, p. 526.
- [10] S. Okada, T. Takada, M. Egashira, J. Yamaki, M. Tabuchi, H. Kageyama, T. Kodama, R. Kanno, in: *Proceedings of the 196th Meeting Abstract of The Electrochemical Society, Hawaii, 1999*.